Psychophysical Measurement of Marmoset Acuity and Myopia

AQ4 Samuel U. Nummela,[1] Shanna H. Coop,[2] Shaun L. Cloherty,[2,3] Chantal J. Boisvert,[4] Mathias Leblanc,[5] Jude F. Mitchell[2]

AQ2 [1] Cortical Systems and Behavior Laboratory, University of California, San Diego

[2] Brain and Cognitive Sciences, University of Rochester, New York

[3] Department of Physiology, Monash University, Melbourne, Australia

[4] Gavin Hebert Eye Institute, University of California, Irvine, California

[5] Animal Resources Department, The Salk Institute, La Jolla, California

Received 7 August 2016; revised 20 October 2016; accepted 21 October 2016

ABSTRACT: The common marmoset has attracted increasing interest as a model for visual neuroscience. A measurement of fundamental importance to ensure the validity of visual studies is spatial acuity. The marmoset has excellent acuity that has been reported at the fovea to be nearly half that of the human (Ordy and Samorajski [1968]: Vision Res 8:1205–1225), a value that is consistent with them having similar photoreceptor densities combined with their smaller eye size (Troilo et al. [2000b]: Vision Res 33:1301–1310). Of interest, the marmoset exhibits a higher proportion of cones than rods in peripheral vision than human or macaque, which in principle could endow them with better peripheral acuity depending on how those signals are pooled in subsequent processing. Here, we introduce a simple behavioral paradigm

similar cortical magnification factor in primary visual cortex (Chaplin et al., 2013). They can also be trained

national primate center. All animals were raised in larger family groups and then pair-housed at maturity.

For several weeks prior to surgery, subjects were acclimated to sit calmly in a small primate chair following methods previously described (Lu et al. 2001; Remington et al. 2012; Osmanski et al. 2013). The design of the primate chair includes a slot that allows the marmoset's tail to hang freely with their weight lifted off their hind quarters, supporting themselves by pressing their lower legs against the inside of the small body tube in which they sit (tube diameter 3 to 3.5 inches). Animals were trained for 2–3 months to sit calmly in the chair without struggle for an extended period, beginning with short intervals of 5 min and building toward a total period of 30–60 min.

All subjects underwent surgery to implant an acrylic head cap with a titanium post that was used to stabilize the

COLOR

Figure 1 Behavioral tasks. (A) A series of frame shots illustrating two sample trials of the Gabor

The Gabor stimulus was always vertically oriented; however spatial frequency and Gabor location was pseudo-randomized over a trials list to construct a psychometric function of spatial frequency sensitivity using the method of constant stimuli. The phase of the Gabor was randomized on each trial.

Within a behavioral session, the eccentricity and size of the Gabor was fixed, however this could vary from session to session (see Table 1, which details conditions of the Gabor task for measurement of acuity for subjects M and S). We tested acuity across a range of values (1.5, 2, 3, 4, 5, 6, 7, 8, 10, and 12 degrees). The order of eccentricity values

T1

tested was pseudo-randomized across sessions with each value being tested at least twice in a separate behavioral session, such that each value was tested in the first half of sessions and then again in the second half of sessions (to reduce any potential training effects). In subject M, we performed tests of two eccentricities each day in a back to back session. In this subject the tested eccentricities were swapped during the collection of

We developed a simple behavioral diagnostic to

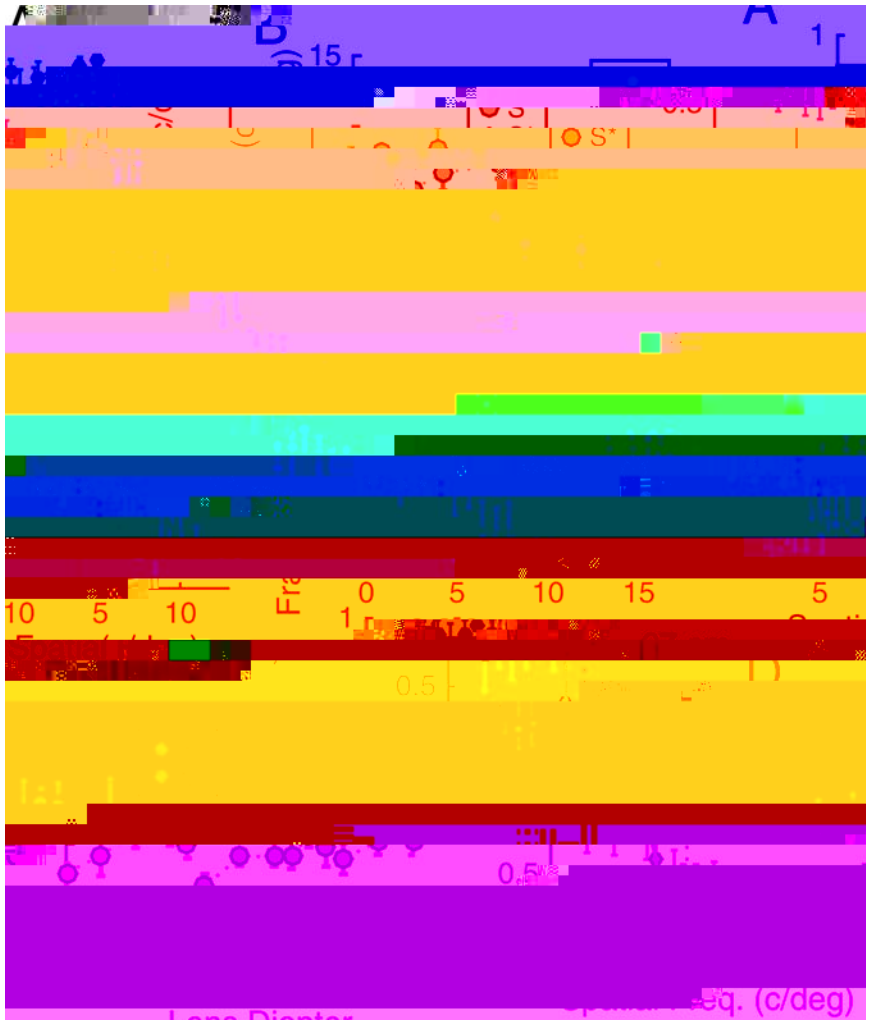

COLOR

Figure 2 Correction of marmoset vision. (A) Plots of the fraction of the detected Gabor stimuli at each spatial frequency sampled, with 95% CIs, for subject M. Display distance is noted by text in each plot. Psychometric fits used to calculate spatial frequency threshold are overlaid as a solid dark gray line. Dotted red reference lines at 7.5 cycles per degree are provided to help compare psychometric fits across plots. (B) Spatial frequency sensitivities as a function of display distance for subjects M (blue) and S (green) are provided by plotting spatial frequency threshold as a function of display distance with 95% CIs from a nonparametric bootstrap. At closer display distances, subject S was also run on an iPad display to increase screen resolution (Brown, denoted S*). (C) A comparison of Gabor detection performance with uncorrected vision (left) and a −3.5 diopter correction (right) for subject M. Raw performance at each spatial frequency with 95% CIs is plotted along with psychometric fits overlaid (solid dark gray lines). A dark grey psychometric fits and a dotted red reference line. Dotted red reference lines are provided at 7.5 cycles per degree. (D) Spatial frequency sensitivities as a function of diopter correction strength at a fixed display distance (90 cm) and retinal eccentricity (4 visual degrees) are summarized for subjects M (blue) and S (green). Error bars are 95% CIs.

for curves that became flat past over-correcting, with the smallest correction giving the same highest performance. We set the correction to −3.50 diopters for subject M, which was a slight over correction from ophthalmologic measurement in Table 2, and −2.00 diopters for subject S, very close to the ophthalmologic measurement. Figure 2(D) also illustrates that this improvement in spatial frequency sensitivity can be very large, even at display distances of less than 100 cm. The threshold for subject M nearly doubled and increased by about 50% for subject S.

With corrected vision, we measured spatial frequency sensitivities at retinal eccentricities ranging from 1.5 to 12 degrees in subject M [Fig. 3(A)] and 2 to 12 degrees in subject S [Fig. 3(B)]. For each measurement, we plotted the raw data of fraction correct at each spatial frequency tested, and overlaid the psychometric fits. Individual data points show 95% confidence intervals of binomial distributions in which magnitude scales with the number of observations, resulting in smaller error bars for greater numbers of observations. The psychometric thresholds for both

this reason, we repeated our measurements of acuity thresholds for subject M at 10 and 12 degrees eccentricity, without correction at a display distance of only 20 cm (close enough to remain in focus for myopia requiring −5 diopter correction). These measurements of acuity threshold were nearly identical to those with correction [Fig. 4(A), subject M*], suggesting that use of the same correction at all eccentrici-

We compared measurements from the marmoset acuity to that of the human and macaque. Figure 4(C) plots a psychophysical measurement of acuity in humans (solid black line, from Berkley et al., 1975) to the psychophysical measurement of marmoset acuity (solid green line). For the marmoset curve, we average the performance of subjects M and S with an additional measurement for central gaze taken from a previous study (Ordy and Samorajski, 1968). Instead of showing a clear inflection point in acuity leveling

photoreceptors in the periphery (Perry and Cowey, 1985), which could reduce the acuity of the retinal input to the rest of the visual system. This has been observed in macaques, in which the density of P-ganglion cells, and not cones, provided a better fit to behavioral acuity (Merigan and Katz, 1990). In Figure 4(D), we compare macaque acuity (solid red line) and Nyquist limits to cone (dotted red line) and P ganglion cell (dotted black line) densities taken from Merigan and Katz to marmoset acuity (solid green line) and Nyquist prediction from marmoset cone density (dotted green line, from Troilo et al., 1993). The Nyquist prediction for the marmoset shows a sharp inflection in slope past 5 degree eccentricity that is not evident for the Nyquist prediction of the macaque (dotted green versus dotted red lines). Nevertheless, the behavioral measurement of marmoset acuity deviates sharply from the Nyquist prediction, just like behavioral measurement of macaque acuity. For the macaque, this deviation can be explained by the higher convergence of cone photoreceptors onto P ganglion cells in the periphery. Our results suggest a similar convergence of cone photoreceptors in marmoset, which is consistent with an early study that reported peripheral pooling was greater in the periphery of the marmoset than in the macaque (Goodchild et al., 1996). Thus, while cone density may be greater in the marmoset periphery, with the greater pooling by retinal ganglion cells in the periphery this higher density is offset. These findings also help explain why the cortical magnification found at the level of visual cortex scales similarly to macaque and human (Chaplin et al., 2013).

One concern is that aliasing in the periphery may increase acuity sensitivity in the detection tasks (Thibos et al., 1996). This could in principle lead to supra-Nyquist detection in the periphery of vision (Williams and Coletta, 1987). We did not observe any signs of supra-Nyquist acuity thresholds in our peripheral data. This may reflect that our most peripheral locations were less eccentric than those of previous studies, or methodological differences such as our choice of display monitor. Of note, measurements of human acuity do not always reflect such peripheral aliasing either, as seen in Figure 4(C) by comparing those measurements using a detection task similar to our own (Berkley et al., 1975) against those measured recently using discrimination tasks of grating orientation that are robust to aliasing (Thibos et al., 1996). Thus while peripheral aliasing may be specific concern for certain test conditions, it does not appear prominent in our data nor could it account for our findings that peripheral acuity thresholds are significantly below the Nyquist limit.

Our findings also emphasize the importance of identifying refractive errors in marmosets prior to conducting visual experiments. One method to diagnose a subject is to perform an ophthalmological refraction, which requires substantial expertise. In subject M and S, we used an alternative set of diagnostics that can be performed using the same simple detection task. First, the presence of myopia can be diagnosed by comparing spatial frequency sensitivity for a fixed retinal eccentricity at two or more distances (such as 29 to 90 cm in the current study). A decrease in the spatial frequency threshold, as seen for subjects M and S [Fig. 2(B)], indicates nearsightedness. In performing this diagnostic, it is important to make sure that the display resolution is sufficient to present the desired stimulus, and this can be particularly challenging for near display distances. In our study, we found aliasing to be an issue with a standard monitor and had to repeat tests with a smaller display for near distances. Typically, 6 pixels per cycle is adequate sampling to ensure a minimal loss of effective stimulus contrast. Using a square wave grating cannot always alleviate this issue, as some light typically escapes from bright pixels into neighboring pixels, resulting in the loss of contrast when only 1 or 2 pixels are alternated in brightness. Second, to find an appropriate correction, we measured the spatial frequency threshold over a range of diopter correction strengths while the display distance remained at a far distance (90 cm). For subjects with myopia, spatial acuity will increase with larger corrections up to some point, where it will either flatten or begin to decline gradually due to the overcorrection [Fig. 2(D)]. Both of these diagnostics made use of the same simple detection task, which required only 1 to 5 training sessions, each an hour long in duration. In applying visual correction, one concern is that measurements at extreme eccentricities might be affected by differences in refractive error between central and peripheral locations (Wang et al., 1997). However, we find no evidence that this affects our results in the near periphery at 10 or 12 visual degrees, based on measurement of acuity threshold using a very near, 20 cm, display distance [Fig. 4(A), M* compared to M]. While most studies in macaque subjects use a display distance of 57 cm as a default, we would instead recommend closer display distances at or below 30 cm in marmoset subjects, unless other means are used to measure and correct myopia.

The incidence of myopia among marmosets raised in captivity is high, and could even be prevalent in natural habitats, and so will generally require correction to ensure the validity of vision studies. Unlike most primate species used in research, which are normally bred and raised in dedicated primate centers,

marmosets are often raised in smaller breeding colonies that may have limited access to distance viewing or natural lighting conditions, which may be a contributing factor. Although rare among macaques used in research, myopia has also been reported in a case study (Mitchell et al., 2014a). Previous studies with marmosets raised in captivity found that mild to severe myopia was common (Graham and Judge, 1999). Consistent with these findings, we observe that all marmosets tested in our study exhibited a significant myopia, ranging from -2 to -4 diopters. Several factors associated with rearing in laboratory conditions could contribute to myopia. One recent study using macaques indicated that indoor lighting

Histed MH, Carvalho LA, Maunsell JHR. 2012. Psychophysical measurement of contrast sensitivity in the behaving mouse. J Neurophysiol 107:758–765.
Kennedy H, Burkhalter A. 2004. Ontogenesis of cortical connectivity. Vis Neurosci 1:146–158.
Kiorpes L. 2015. Visual development in primates: Neural mechanisms and critical periods. Dev Neurobiol 75: 1080–1090.
Kiorpes L, Bassin SA. 2003. Development of contour integration in macaque monkeys. Vis Neurosci 20:567–575.
Kiorpes L, Movshon A, Chaluppa W. 2014. Neuronal limitations on visual development in primates: Beyond striate cortex.
Kleiner M, Brainard D, Pelli D, Ingling A, Murray R, Broussard C. 2007. What's new in Psychtoolbox-3. Perception 36:1.
Lu T, Liang L, Wang X. 2001. Neural representations of temporally asymmetric stimuli in the auditory cortex of awake primates. J Neurophysiol 85:2364–2380.
Merigan WH, Katz LM. 1990. Spatial resolution across the macaque retina. Vision Res 30:985–991.
Miller CT, Freiwald WA, Leopold DA, Mitchell JF, Silva AC, Wang X. 2016. Marmosets: A neuroscientific model of human social behavior. Neuron 90:219–233.
Mitchell JF, Boisvert CJ, Reuter JD, Reynolds JH, Leblanc M. 2014a. Correction of refractive errors in rhesus macaques (*Macaca mulatta*) involved in visual research. Comp Med 64:300–308.
Mitchell JF, Leopold DA. 2015. The marmoset monkey as a model for visual neuroscience. Neurosci Res 93:20–46.
Mitchell JF, Reynolds JH, Miller CT. 2014b. Active vision in marmosets: A model system for visual neuroscience. J Neurosci 34:1183–1194.
Movshon JA, Kiorpes L. 1988. Analysis of the development of spatial contrast sensitivity in monkey and human infants. J Opt Soc Am A 5:2166–2172.
Nickla DL, Wildsoet CF, Troilo D. 2002. Diurnal rhythms in intraocular pressure, axial length, and choroidal thickness in a primate model of eye growth, the common marmoset. Invest Ophthalmol Vis Sci 43:2519–2528.
Ordy JM, Samorajski T. 1968. Visual acuity and ERG-CFF in relation to the morphologic organization of the retina among diurnal and nocturnal primates. Vision Res 8:1205–1225.
Osmanski MS, Song X, Wang X. 2013. The role of harmonic resolvability in pitch perception in a vocal nonhuman primate, the common marmoset (*Callithrixjacchus*). J Neurosci 33:9161–9168.
Pelli DG. 1997. The VideoToolbox software for visual psychophysics: Transforming numbers into movies. Spat Vis 10:437–442.
Perry VH, Cowey A. 1985. The ganglion cell and cone distributions in the monkey's retina: Implications for central magnification factors. Vision Res 25:1795–1810.
Prins N, Kingdom FAA. 2009. Palamedes: Matlab routines for analyzing psychophysical data.

AQ1: Please confirm whether short title is OK as typeset.

AQ2: Please provide department/division for 1, 2, 4, 5 affiliations.

AQ3: Please provide complete details for references “Kiorpes L, Movshon A, Chaluppa W. 2014; Prins N, Kingdom FAA. 2009.”

AQ4: Please confirm that given names (red) and surnames/family names (green) have been identified correctly.

Please confirm that the funding sponsor list below was correctly extracted from your article: that it includes all
